The $\gamma^\star\gamma \to \pi^0$ transition in a bound-state approach [a]

DUBRAVKO KLABUČAR

Physics Department, Faculty of Science, University of Zagreb,
Bijenička c. 32, Zagreb, Croatia

DALIBOR KEKEZ

Rudjer Bošković Institute, POB 1016, 10001 Zagreb, Croatia

We present a recent treatment of the $\pi^0\gamma^\star\gamma$ transition form factor in the coupled Schwinger-Dyson and Bethe-Salpeter approach to stress the desirability of measuring it at CEBAF.

The form factor $T_{\pi^0}(-Q^2, 0)$ for the transition $\gamma^\star(k)\gamma(k') \to \pi^0(p)$ (where $k^2 = -Q^2 \neq 0$ is the momentum-squared of the spacelike off-shell photon $\gamma^\star$), is usually thought to be almost completely understood on the basis of the perturbative QCD (pQCD) over the whole range of the momenta-squared covered by the new CLEO data [1] (1.5 GeV$^2 \lesssim Q^2 \lesssim 9$ GeV^2). However, Radyushkin and Ruskov's [2] QCD sum rule analysis indicates the presence of large nonperturbative contributions even for the largest of these presently accessible momenta. This motivated us to address in Ref. [3] the transition form factor in the coupled Schwinger–Dyson (SD) and Bethe–Salpeter (BS) approach in all spacelike-momentum regimes, from very large Q^2 all the way to $Q^2 = 0$. The $Q^2 = 0$ limit corresponds to the π^0 decay into two real photons ($k^2 = k'^2 = 0$) explained by the Abelian axial *alias* Adler-Bell-Jackiw (ABJ) anomaly, which is usually difficult to incorporate into a bound-state approach [4]. Fortunately, as shown already in Refs. [5,6] and used in the first analysis of $T_{\pi^0}(-Q^2, 0)$ in a SD approach [7], such approaches which rely on the chirally well–behaved SD (and BS) equations for the light pseudoscalar mesons ($\pi, K, \eta, ...$) while respecting the Ward-Takahashi identities (WTI) of QED, reproduce (in the chiral and soft limit) the fundamental anomaly result

$$T_{\pi^0}(0,0) = \frac{1}{4\pi^2 f_\pi} \tag{1}$$

naturally and without any fine tuning. This is an advantage with respect to pQCD approaches, which have problems at low Q^2. (*E.g.*, see Ref. [8].)

---

[a] The talk given by D. Klabučar at Semi-Exclusive Workshop, Jefferson Lab, May 19–22, 1999. To appear in the proceedings of the Workshop.

In the present coupled SD-BS approach [4, 9, 10], the anomalous amplitude (1) is also obtained model-independently and without imposing any requirements on the solutions for the π^0 wave function or the quark propagator solutions (*e.g.*, see [5, 6]). This is exactly as it should be, since the anomaly – and its result (1) – must not depend on the internal structure of the pion. Subsequently, in Ref. [3], we showed that the SD-BS approach to modeling QCD provides a good description for *both* low and high values of Q^2. We thereby obtained the behavior similar to the Brodsky–Lepage interpolation formula $T_{\pi^0}(-Q^2, 0) = (1/4\pi^2 f_\pi) / (1 + Q^2/8\pi^2 f_\pi^2)$ proposed [11] as a desirable behavior for $T_{\pi^0}(-Q^2, 0)$ as it reduces to the ABJ anomaly amplitude (1) at $Q^2 = 0$, while agreeing with the following type of leading behavior for large Q^2:

$$T_{\pi^0}(-Q^2, 0) = \mathcal{J} \frac{f_\pi}{Q^2} \qquad (\mathcal{J} = constant \text{ for large } Q^2), \qquad (2)$$

which is favored both experimentally [1] and theoretically (*e.g.*, [2, 8, 11, 12]).

In the coupled SD-BS approach, the BS equation for the pion bound-state $q\bar{q}$ vertex $\Gamma_{\pi^0}(q, p)$ employs the dynamically dressed quark propagator $S(k) = [A(k^2)\slashed{k} - B(k^2)]^{-1}$, obtained by solving its SD equation. Then, in the case of light pseudoscalars, the $q\bar{q}$ bound states are simultaneously also the (pseudo-)Goldstone bosons of dynamical chiral symmetry breaking (DχSB).

Following Jain and Munczek [13, 14], we adopt the ladder-type approximation employing bare quark–gluon–quark vertices but dressed propagators. For the gluon propagator we use an effective, (*partially*) modeled one in Landau-gauge [13, 14], given by $G(-l^2)(g^{\mu\nu} - l^\mu l^\nu/l^2)$. (This Ansatz is often called the "Abelian approximation" [15].) The effective propagator function G is the sum of the perturbative contribution G_{UV} and the nonperturbative contribution G_{IR}: $G(Q^2) = G_{UV}(Q^2) + G_{IR}(Q^2)$, $(Q^2 = -l^2)$. The perturbative part G_{UV} is required to reproduce correctly the ultraviolet (UV) asymptotic behavior that unambiguously follows from QCD in its high–energy regime. Therefore, G_{UV} must be given by $\alpha_s(Q^2)/Q^2$, where the running coupling constant $\alpha_s(Q^2)$ is well-known from pQCD, so that G_{UV} is *not* modeled. As in Refs. [4, 9, 10], we follow Refs. [13, 14] and employ the two–loop asymptotic expression for $\alpha_s(Q^2)$. For the modeled, IR part, we adopt from Ref. [14] $G_{IR}(Q^2) = (16\pi^2/3) \, a \, Q^2 e^{-\mu Q^2}$ and $a = (0.387\,\text{GeV})^{-4}$, $\mu = (0.510\,\text{GeV})^{-2}$.

Our calculational procedures are detailed in our Refs. [4, 9, 10]. We reproduce the solutions of Ref. [14] for the dressed propagator $S(q)$, *i.e.*, $A(q^2)$ and $B(q^2)$, as well as the solutions for the four functions comprising the pion bound-state vertex Γ_{π^0}. Actually, Ref. [14] employs the BS amplitude $\chi_{\pi^0}(q, p) \equiv S(q + p/2)\Gamma_{\pi^0}(q, p)S(q - p/2)$, which is completely equivalent.

We assume that the $\pi^0\gamma^\star\gamma$ transition (and other pseudoscalar meson $\rightarrow$
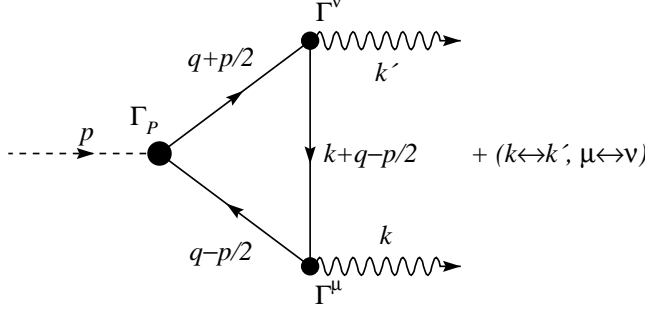
Figure 1: The GIA diagram for $P^0 \to \gamma^{(\star)}\gamma^{(\star)}$ processes ($P^0 = \pi^0, \eta, \eta', \eta_c, \eta_b$).

two photon transitions) proceeds through the pseudoscalar-vector-vector triangle graph (Fig. 1), and that we calculate the pertinent amplitude $T^{\mu\nu}_{\pi^0}(k, k') = \varepsilon^{\alpha\beta\mu\nu} k_\alpha k'_\beta T_{\pi^0}(k^2, k'^2)$ as in Refs. [4, 9, 10], using the framework advocated by, *e.g.*, Refs. [5–7] in the context of electromagnetic interactions of BS bound states, and often called (*e.g.*, by Ref. [7]) the generalized impulse approximation (GIA). We therefore use the *dressed* quark propagator $S(q)$ and the pseudoscalar BS bound–state vertex $\Gamma_P(q, p)$, as well as consistently dressed *electromagnetic* vertex $\Gamma^\mu(q', q)$, which satisfies the vector Ward–Takahashi identity (WTI) $(q' - q)_\mu \Gamma^\mu(q', q) = S^{-1}(q') - S^{-1}(q)$. Namely, assuming that photons couple to quarks through the bare vertex γ^μ would be inconsistent with our dressed quark propagator $S(q)$, which contains the momentum-dependent functions $A(q^2)$ and $B(q^2)$. The bare vertex γ^μ obviously violates the vector WTI, implying the nonconservation of the electromagnetic vector current and charge. Solving the pertinent SD equation for the dressed quark–photon–quark ($qq\gamma$) vertex Γ^μ is still an unsolved problem, and using the realistic Ansätze for Γ^μ still remains the only practical way to satisfy the WTI. The simplest particular solution of the vector WTI is the Ball–Chiu (BC) [16] vertex

$$\Gamma^\mu_{BC}(q', q) = A_+(q'^2, q^2)\frac{\gamma^\mu}{2} + \frac{(q' + q)^\mu}{(q'^2 - q^2)}\{A_-(q'^2, q^2)\frac{(\slashed{q}' + \slashed{q})}{2} - B_-(q'^2, q^2)\} \ , \quad (3)$$

where $H_\pm(q'^2, q^2) \equiv [H(q'^2) \pm H(q^2)]$, for $H = A$ or B. It does *not* introduce any new parameters as it is completely determined by the dressed quark propagator $S(q)$. In the SD-BS approach, this minimal WTI-satisfying Ansatz (3) is still the most widely used $qq\gamma$ vertex (*e.g.*, Refs. [6,7,9,10]). A general WTI-

3

satisfying vertex can be written [16] as $\Gamma^\mu = \Gamma_{BC}^\mu + \Delta\Gamma^\mu$, where the addition $\Delta\Gamma^\mu$ doesn't contribute to the WTI, since it is transverse, $(q'-q)_\mu \Delta\Gamma^\mu(q',q) = 0$. That is, $\Delta\Gamma^\mu(q',q)$ lies in the hyperplane spanned by the vectors $\mathcal{T}_i^\mu(q',q)$ $(i = 1,...,8)$ transverse to the photon momentum $k = q' - q$. Curtis and Pennington (CP) [17] advocated an Ansatz for $\Delta\Gamma^\mu(q',q)$ exclusively along the $i = 6$ basis vector: $\Delta\Gamma^\mu(q',q) = \mathcal{T}_6^\mu(q',q)[A_-(q'^2,q^2)/2d(q',q)]$. The coefficient of $\mathcal{T}_6^\mu(q',q)$ can be chosen to ensure renormalizability [17], $e.g.$,

$$ d_\pm(q',q) = \frac{1}{q'^2 + q^2} \left\{ (q'^2 \pm q^2)^2 + \left[M^2(q'^2) + M^2(q^2) \right]^2 \right\} , \qquad (4) $$

where $M(q^2) \equiv B(q^2)/A(q^2)$ is the DχSB-generated dynamical mass function, which in our case has the large-q^2 dependence [4] in agreement with pQCD.

The choice $d = d_-$ corresponds to the CP vertex Ansatz Γ_{CP}^μ [17]. We use it in analytic calculations of $T_{\pi^0}(-Q^2,0)$, which are possible for $Q^2 = 0$ and $Q^2 \to \infty$. However, in the numerical calculations, which are necessary for finite values of $Q^2 \neq 0$, we prefer the $modified$ CP (mCP) vertex, Γ_{mCP}^μ [3], resulting from the choice $d = d_+$, since it is easier to deal with numerically. Unlike the BC one, the mCP vertex is consistent with renormalizability just like the CP one. In the present context, the important $qualitative$ difference between the BC vertex, and the CP as well as the modified, mCP vertex, is that $\Gamma_{BC}^\mu(q',q) \to \gamma^\mu$ when $both$ $q'^2, q^2 \to \pm\infty$, whereas $\Gamma_{CP}^\mu(q',q) \to \gamma^\mu$ and $\Gamma_{mCP}^\mu(q',q) \to \gamma^\mu$ as soon as one of the squared momenta tends to infinity.

Assuming the isospin symmetry, $\chi \equiv \chi_{u\bar{u}} = \chi_{d\bar{d}}$ is the BS amplitude for both $u\bar{u}$ and $d\bar{d}$ pseudoscalar bound states, and $\chi_{\pi^0}(q,p) \equiv \chi(q,p)\lambda^3/\sqrt{2}$. Then, for π^0, GIA yields (see Fig. 1) the tensor amplitude

$$ T_{\pi^0}^{\mu\nu}(k,k') = -N_c \frac{1}{3\sqrt{2}} \int \frac{d^4q}{(2\pi)^4} \text{tr}\{\Gamma^\mu(q - \frac{p}{2}, k + q - \frac{p}{2})S(k + q - \frac{p}{2}) $$

$$ \times \Gamma^\nu(k + q - \frac{p}{2}, q + \frac{p}{2})\chi(q,p)\} + (k \leftrightarrow k', \mu \leftrightarrow \nu), \qquad (5) $$

leading to the analytical reproduction of the $\pi^0 \to \gamma\gamma$ amplitude (1) with the CP and mCP vertices, in the same way as with the BC vertices.

Let us stress that in the regime of asymptotically large Q^2, we obtained [3] analytical results for the transition form factor in agreement with the behavior (2). Since the pion is light, $k \cdot k' \approx Q^2/2$ for large negative $k^2 = -Q^2$ and $k'^2 = 0$. Taking into account the behavior of the propagator functions $A(q^2)$ and $B(q^2)$ ($e.g.$, see [4]) we can then in Eq. (5) approximate those quark propagators that depend on the photon momenta k and k', by their asymptotic forms: $S(q - p/2 + k) \approx S(k - p/2) \approx -(2/Q^2)(\not{k} - \not{p}/2)$

4

and analogously for the propagator where k is replaced by k'. Although the relative loop momentum q can be large in the course of integration, its neglecting is justified because the BS amplitude $\chi(q,p)$ decays quickly and thus strongly damps the integrand for the large q's. Ref. [3] then showed that $T^{\mu\nu}_{\pi^0}(k,k') = -(2/N_c\,Q^2)\,\varepsilon^{\mu\lambda\nu\sigma}(k-k')_\lambda p_\sigma\, f_\pi$, finally leading to Eq. (2) with the coefficient $\mathcal{J} = 4/3$. We thus found *model independently* that the asymptotic behavior in the present approach (with $qq\gamma$ vertices such as the bare γ^μ, mCP and CP), agrees exactly with the leading term predicted by OPE [12].

The asymptotic behavior $\propto 1/Q^2$ obtained in the present approach is especially satisfying when compared with the one known to result from the simple constituent quark model (with the constant light–quark mass parameter m_u), where $T_{\pi^0}(-Q^2,0) \propto (m_u^2/Q^2)\ln^2(Q^2/m_u^2)$ as $Q^2 \to \infty$, which overshoots the data considerably because of the additional $\ln^2(Q^2)$-dependence.

It is important to note that this asymptotic behavior, $T_{\pi^0}(-Q^2,0) = (4/3)f_\pi/Q^2$, was obtained for the $qq\gamma$ vertices which reduce to the bare one, γ^μ, as soon as *one* of the squared momenta tends to infinity, such as the renormalizable CP and mCP vertices. Subsequently, Ref. [18] showed that this asymptotic behavior must in fact hold for *any* renormalizable $qq\gamma$ vertex. For the simplest dressed WTI-preserving vertex, the BC one, which reduces to the bare one only when momenta are large in both of its fermion legs, and which is not consistent with multiplicative renormalizability [17], the asymptotic behavior is $(4/3)\widetilde{f}_\pi/Q^2$, where the quantity $\widetilde{f}_\pi$ is given by the same Mandelstam-formalism expression as f_π except that its integrand is modified by the factor $[1 + A(q^2)]^2/4$ [3]. For our model solutions [4], $\widetilde{f}_\pi \approx 1.334 f_\pi$, so that the usage of the BC vertices causes the increase of $\mathcal{J}$ in Eq. 2 from $\mathcal{J} = 4/3$ to $\mathcal{J} \approx 1.78$.

Of course, the model-independent asymptotic coefficient $4f_\pi/3$ is the one having the more fundamental meaning, resulting from the renormalizable $qq\gamma$ vertices such as the CP or mCP ones, which have properties closer to the true vertex solution. Also indicative is the asymptotics found [3] for such $qq\gamma$ vertices when both photons are off-shell, $k^2 = -Q^2 << 0$ and $k'^2 = -Q'^2 \leq 0$:

$$T_{\pi^0}(-Q^2,-Q'^2) = \frac{4}{3}\frac{f_\pi}{Q^2 + Q'^2}\,. \tag{6}$$

The usage of the BC vertex (3) would again modify this result by the substitution $f_\pi \to \widetilde{f}_\pi$. However, Eq. (6) agrees with the leading term of the OPE result of Novikov *et al.* [19] for the special case $Q^2 = Q'^2$. Also, the distribution-amplitude-dependence of the pQCD approach cancels out for that symmetric case, so that $T_{\pi^0}(-Q^2,-Q'^2)$ in this approach (*e.g.*, see [20]), in the limit $Q^2 = Q'^2 \to \infty$, exactly agrees with both our Eq. (6) and Ref. [19]. For that symmetric case, we should thus have even the precise agreement of

the coefficients irrespective of the description of the pion internal structure en-
coded in the distribution amplitude. Obviously, this favors the renormalizable
$qq\gamma$ vertices, such as CP and mCP ones, over the BC vertex. However, the
BC vertex may anyway be the one which is more accurate not only for the
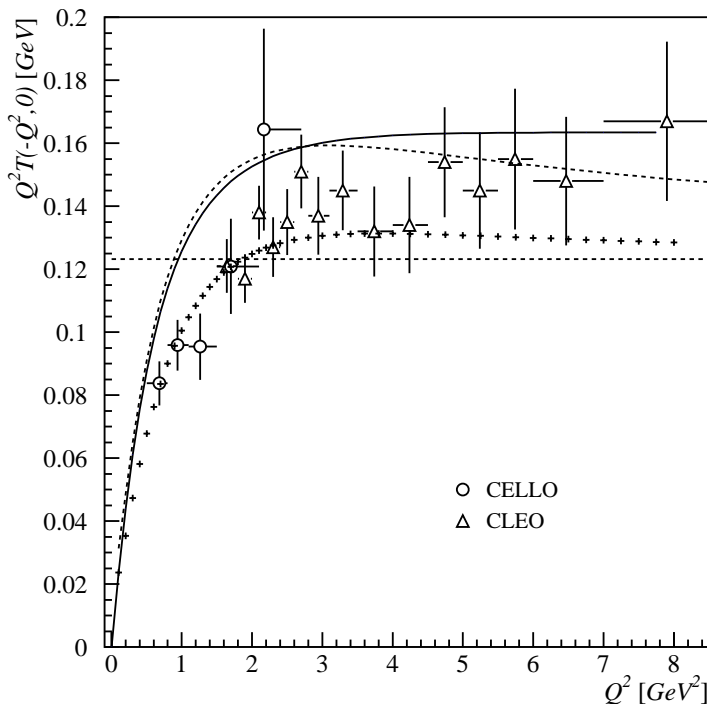presently accessible Q^2, but also for larger values before starting to fail.

Figure 2: Our numerically obtained $Q^2 T_{\pi^0}(-Q^2, 0)$ and the data.

For finite Q^2, the transition form factor is evaluated numerically. Fig. 2
compares so obtained $Q^2 T_{\pi^0}(-Q^2, 0)$ with the CLEO [1] and CELLO [21] data.
The solid curve is obtained with the BC vertices, and the dashed curve with
the mCP ones. The horizontal dashed line denotes $4f_\pi/3$, the asymptotic value
for renormalizable $qq\gamma$ vertices such as the mCP one. It barely touches the
experimental error bars from below. Note that also Manohar [12] warned that
his OPE approach (also yielding $4f_\pi/3$) indicates the possibility of large correc-
tions to his leading term, but possibly also to the pQCD asymptotic coefficient
$2f_\pi$, which is however exact in the $strict \ln(Q^2) \to \infty$ limit [11]. We get it lower

by the factor 2/3 because our present approach does not incorporate the effects of the pQCD evolution. However, as Ref. [2] seems to indicate that effects other than the pQCD evolution (including the presently interesting dynamical dressing of quarks) may still play important (and maybe even dominant) role even at Q^2-values larger than the presently accessible ones, one should consider seriously also nonperturbative approaches such as ours. On the other hand, high-precision measurements of $T_{\pi^0}(-Q^2, 0)$ can test (and give a hint on how to improve) the SD and BS model solutions which have so far been successful in fitting the low-energy hadron properties such as the meson spectrum. For example, our model choice [14] somewhat overshoots (for both BC and mCP vertices) the present $T_{\pi^0}(-Q^2, 0)$ data [1, 21] in the region $Q^2 \lesssim 4$ GeV^2.

Once one has a solution for $\chi(q, p)$ that leads to the correct value of f_π, the transition form factor is most sensitive on $A(q^2)$, or, more precisely, on its values at small and intermediate momenta $-q^2$, where $A(q^2)$ is still appreciably different from 1 [3, 22]. To illustrate what happens when the $A(q^2)$-profile is decreased, let us enforce by hand the extreme, artificial case $A(q^2) \equiv 1$. (To avoid confusion, we stress it is for illustrative purposes only, as we cannot have such a SD-solution in the adopted approach of Refs. [13, 14].) This leads to the curve traced on Fig. 2 by small crosses, pertaining to the usage of both BC and mCP vertices (as well as the CP ones), since $A(q^2) \equiv 1$ makes $\Gamma^\mu_{mCP} \to \Gamma^\mu_{BC}$. This curve reveals how the heights of the curves depicting $Q^2 T_{\pi^0}(-Q^2, 0)$ depend on how much the $A(q^2)$-profile exceeds 1. Obviously, for both the solid curve and the dashed one, the agreement with experiment would be improved by lowering them somewhat (at least in the momentum region $Q^2 \lesssim 4$ GeV), which could be achieved by modifying the model [14] and/or its parameters so that such a new solution for $A(q^2)$ is somewhat lowered towards its asymptotic value $A(q^2 \to \infty) \to 1$. (Of course, in order to be significant, this must not be a specialized re-fitting aimed *only* at $A(q^2)$. Lowering of $A(q^2)$ should be a result of a broad fit to many meson properties, comparable to the original fit [14]. This, however, is beyond the scope of this paper.)

By the same token, high precision measurements of $T_{\pi^0}(-Q^2, 0)$ can be especially helpful in obtaining information on which solutions for $A(q^2)$ are empirically acceptable and which are not. Of course, measurements of $T_{\pi^0}(-Q^2, 0)$ give information on the integrated strength of $A(q^2)$ rather than on $A(q^2)$ itself. However, since it is known that the form of that function must be a rather smooth transition (*e.g.*, see [4]) from $A(q^2) > 1$ for q^2 near 0, to $A(q^2) \to 1$ in the q^2-domain where QCD is perturbative, such measurements [23] would give a useful hint even about $A(q^2)$ itself – namely about what solutions for $A(q^2)$ one may have in sensible descriptions of dynamically dressed quarks and their

bound states. Therefore, the intermediate-momentum ($Q^2 \lesssim 4$ GeV^2) measurements of $T_{\pi^0}(-Q^2, 0)$ at Jefferson Lab, such as those proposed in Ref. [23], would be very desirable. Hopefully, the study of virtual Compton scattering at CEBAF can produce the data on $T_{\pi^0}(-Q^2, 0)$ as envisioned in Ref. [23].

Acknowledgments

References

1. J. Gronberg *et al.* (CLEO collaboration), Phys. Rev. D **57**, 33 (1998).
2. A. V. Radyushkin and R. T. Ruskov, Nucl. Phys. B **481**, 625 (1996).
3. D. Kekez and D. Klabučar, Phys. Lett. **457B**, 359 (1999).
4. D. Kekez *et al.*, Int. J. Mod. Phys. A **14**, 161 (1999).
5. M. Bando, M. Harada, and T. Kugo, Prog. Theor. Phys. **91**, 927 (1994).
6. C. D. Roberts, Nucl. Phys. A **605**, 475 (1996).
7. M.R. Frank *et al.*, Phys. Lett. B **359**, 17 (1995).
8. I. V. Musatov and A. V. Radyushkin, Phys. Rev. D **56**, 2713 (1997).
9. D. Kekez and D. Klabučar, Phys. Lett. B **387**, 14 (1996).
10. D. Klabučar and D. Kekez, Phys. Rev. D **58**, 096003 (1998).
11. G. P. Lepage and S. J. Brodsky, Phys. Rev. D **22**, 2157 (1980).
12. A. Manohar, Phys. Lett. **B244**, 101 (1990).
13. P. Jain and H. J. Munczek, Phys. Rev. D **44**, 1873 (1991); Phys. Rev. D **46**, 438 (1992).
14. P. Jain and H. J. Munczek, Phys. Rev. D **48**, 5403 (1993).
15. P. Maris and C. D. Roberts, Phys. Rev. C **56**, 3369 (1997).
16. J. S. Ball and T.-W. Chiu, Phys. Rev. D **22**, 2542 (1980).
17. D. C. Curtis and M. R. Pennington, Phys. Rev. D **42**, 4165 (1990).
18. C. D. Roberts, Fizika B (Zagreb) **8**, 285 (1999).
19. V. A. Novikov *et al.*, Nucl. Phys. B **237**, 525 (1984).
20. P. Kessler and S. Ong, Phys. Rev. D **48**, R2974 (1993).
21. H.-J. Behrend *et al.* (CELLO Collaboration), Z. Phys. C **49**, 401 (1991).
22. D. Klabučar and D. Kekez, Fizika B (Zagreb) **8**, 303 (1999).
23. CEBAF Letter of Intent # LOI–94/005. Co–Spokesmen: A. Afanasev, J. Gomez, and S. Nanda; A. Afanasev, `hep-ph/9608305`.